(10) Sushchinski, M. M. *Raman Spectra of Molecules and Crystals*; Israel Program for Scientific Translation Ltd.; 1972; 186.
(11) Stanley, K.; Freeman, *Application of Laser Raman Spectroscopy*; Wiley: New York, 1974; p 125.
(12) Sandman, D. J.; Chen, Y. J.; Elman, B. S.; Velazquez, C. S. *Macromolecules* **1988**, *21*, 3112.
(13) (a) Stanly, J.; Smith, D.; Latimer, B.; Devlin, J. *J. Phys. Chem.* **1966**, *70* (6), 2011. (b) Harada, I.; Tasumi, M.; Shirakawa, H.; Ikeda, S. *Chem. Lett.* **1978**, 1411. (c) Rabolt, J. F.; Clarke, T. C.; Street, G. B. *J. Chem. Phys.* **1979**, *71* (11), 4614.
(14) (a) Fincher, C. R., Jr.; Peebles, D. L.; Heeger, A. J.; Druy, M. A.; Matsamura, Y.; MacDiarmid, A. G.; Shirakawa, H.; Ikeda, S. *Solid State Commun.* **1978**, *27*, 489. (b) Shirakawa, H.; Sasaki, T.; Ikeda, S. *Chem. Lett.* **1978**, 1113.
(15) (a) Epstein, A. J.; Rommelmann, H.; Fernquist, R.; Gibson, H. W. *Polymer* **1982**, *23*, 1211. (b) Rommelman, H.; Ferquist, R.; Gibson, H. W.; Epstein, A. J.; Druy, M. A.; Woener, T. *Mol. Cryst. Liq. Cryst.* **1981**, *77*, 177. (c) Marc, J. M. A.; Sidi, M. B. H.; Michel, C.; Michel, R. *Polymer* **1986**, *27*, 2003.
(16) Nechtstein, M.; Devreux, F.; Genoud, F.; Guglielmi, M.; Holczer, K. *Phys. Rev. B* **1983**, *27*, 61.

Registry No. DPDPM (homopolymer), 127974-83-8; WCl_6, 13283-01-7; $MoCl_5$, 10241-05-1; $(n\text{-}Bu)_4Sn$, 1461-25-2; $PdCl_2$, 7647-10-1; $EtAlCl_2$, 563-43-9; Et_2AlCl, 96-10-6; I_2, 7553-56-2.

Cholesteric Helical Pitch of Near Persistence Length DNA

David H. Van Winkle,*,† Michael W. Davidson,‡ Wan-Xu Chen,‡ and Randolph L. Rill*,‡

Department of Physics and Center for Materials Research and Technology and Department of Chemistry and Institute of Molecular Biophysics, The Florida State University, Tallahassee, Florida 32306-3006

Received September 5, 1989; Revised Manuscript Received March 7, 1990

ABSTRACT: Simple aqueous solutions of DNA, a semirigid, strong polyelectrolyte, at high concentration in a 1:1 supporting electrolyte medium, undergo a series of transitions between anisotropic phases including a cholesteric liquid-crystalline phase with a pitch of ≈ 2 μm.[19] Measurements were made, by polarized light microscopy and laser light diffraction, of the cholesteric helical pitch in buffered aqueous solutions of DNA molecules with a contour length near the persistence length (500 Å) as a function of increasing DNA concentration, 1:1 supporting electrolyte concentration, and ionic species. The lowest density anisotropic DNA phase, termed precholesteric, exhibited weakly birefringent periodicities with a spacing strongly dependent on local DNA concentration, ranging from 10 to 50 μm. As the DNA concentration was increased, a highly regular cholesteric phase with a pitch of ≈ 2 μm came into coexistence with the precholesteric phase, and ultimately the solutions became fully cholesteric. No change in pitch of this cholesteric was noted with increasing DNA concentration or ionic strength over a DNA concentration range of $\approx$130–300 mg/mL and a supporting electrolyte concentration of 0.01–1.0 M NaCl. Transition to a high-density phase at DNA concentration > 300 mg/mL was preceded by unwinding of the pitch from 2.2 ± 0.2 to >10 μm. The constant ≈ 2-μm-pitch cholesteric phase was stable to higher DNA concentrations when sodium rather than ammonium was the principal counterion. These results are discussed in the context of theories of the phase behavior of lyotropic liquid crystals of chiral rods.

Introduction

The formation of ordered, liquid-crystal-like phases in biological systems has been the focus of a growing number of studies (reviewed in refs 1–5). There is strong electron microscopic evidence that DNA, in particular, exists in cholesteric-like liquid-crystalline phases in the chromosomes of dinoflagellates and other primitive organisms.[6] A lamellar phase has also been proposed for DNA packing in certain virus capsids.[7]

Onsager,[8] Flory,[9,10] and others[11,12] showed as long as 40 years ago that ordering of solutions of rodlike molecules and semirigid polymers in good solvents is expected above some critical volume fraction because of requirements for minimizing the polymer excluded volume. For nonchiral, uncharged rods this is manifested by an isotropic to nematic liquid-crystalline phase transition. DNA rods are both highly charged and inherently chiral; hence, it is expected and observed that at least one of the ordered DNA phases is cholesteric, i.e., exhibits a long-wavelength twist of the molecular director along a single axis. Odijk and co-workers have recently examined the theoretical basis for forming a cholesteric phase in solutions of charged rod polymers (reviewed in ref 13).

Observations of liquid-crystalline DNA (lcDNA) phases in vitro date to the early 1960s when Robinson showed by polarized light microscopy that relatively high molecular weight DNA solutions spontaneously form cholesteric-like liquid-crystalline phases as the DNA concentration is increased.[14] Cholesteric-like phases have been described subsequently for a number of other double-stranded DNA and RNA systems.[4,15-32] Maret and co-workers[20,21] examined the cholesteric phase of polydisperse poly(A)·poly(U) ribonucleic acid duplexes with an average length of about 1700 Å by small-angle neutron scattering, light diffraction from magnetically oriented samples, and measurements of the magnetic birefringence. Iizuka and co-workers investigated the isotropic to cholesteric

* Authors to whom correspondence should be sent.
† Department of Physics and Center for Materials Research and Technology.
‡ Department of Chemistry and Institute of Molecular Biophysics.

0024-9297/90/2223-4140$02.50/0

transition in polydisperse polyribonucleotide complexes as well as high molecular weight DNA samples.[22-26] In addition, Livolant, Bouligand, and their co-workers have described a number of light and electron microscopic studies of the phases formed by various biological polymers (including DNA) in solution[27-30] and have observed cholesteric phases in polydisperse samples of DNA, poly(benzyl L-glutamate) (PBLG, a rodlike polypeptide), and xanthin (a rodlike polysaccharide).

Recently we showed that relatively monodisperse DNA fragments with a contour length (500 Å) near the persistence length in simple aqueous solutions of a 1:1 electrolyte undergo a complex series of phase changes and form at least three distinct liquid-crystal phases, which appear strongly analogous to phases formed by certain thermotropic and lyotropic small molecules.[16-19] The lowest density anisotropic DNA phase has been termed *precholesteric*. This phase is poorly characterized but appears to be a twisted nematic with a very long pitch. A second, higher density phase has a well-defined cholesteric pitch of approximately 2 μm. A third, yet higher density phase possesses additional order and exhibits microscopic textures analogous to certain smectic and columnar phases assumed by small molecules. Livolant et al. have recently presented data indicating that this phase is columnar hexagonal.[33]

A phase diagram (concentration vs temperature from 20 to 70 °C, the limit of DNA stability) for the isotropic → biphasic and biphasic → liquid-crystalline DNA transitions in 0.3 M NaCl has been determined by solid-state ^{31}P NMR methods.[18] This phase diagram is in good agreement with predictions of the lattice statistics theory of Flory[9,10] for had rods assuming that these short DNA molecules can be treated as rigid rods with a scaled effective hard-core radius of 22 Å at this supporting electrolyte concentration. The radius is consistent with calculations of the effective DNA radius based on polyelectrolyte theories.[34-38] Additional phase-transition data for Na^+DNA have also been obtained at supporting electrolyte concentrations of C^+ = 0.01, 0.1, and 1.0 M (NaCl) (Strzelecka and Rill[37] and manuscripts in preparation).

We report here an investigation, by laser light diffraction and polarized light microscopy, of the variation of the cholesteric pitch with DNA concentration (C_D), supporting electrolyte concentration (C^+), and counterion type (Na^+ or NH_4^+). On the basis of prior results,[20-22] it was expected that the pitch would *decrease* with increasing C_D. We observed instead that the pitch was relatively independent of C_D and C^+ over wide ranges but *increased* with concentration approaching the cholesteric → high-density phase transition.

Experimental Section

Isolation of DNA and Preparation of Liquid-Crystalline DNA. Nucleosome core-length (approximately 500 Å) DNA was isolated from calf thymus chromatin and purified as previously described.[18] To concentrate the DNA, a 10 mg/mL DNA sample, dialyzed into the appropriate buffer, was filtered through a 0.4-μm Nylon filter and placed in a collodion bag (Schleicher and Schuell, no. 43-25320) and immersed in buffer under reduced pressure. This method of concentrating DNA assures maintenance of supporting electrolyte concentration and yields DNA samples ranging in concentration from 100 to 150 mg/mL. Further concentration was achieved by placing the collodion bag in a beaker containing dry cross-linked polyacrylamide beads (Bio-Rad Laboratories, Bio-Gel P-300) for varying lengths of time. A micro stirring bar was placed into the collodion bag to provide mixing during concentration, and 100-μL aliquots of lcDNA were removed from the bag in 15-min intervals. DNA concentrations were determined by diluting 50-μL aliquots of the lcDNA sample into buffer and measuring the absorbance at 260 nm and assuming an extinction coefficient of 6600 M^{-1} DNA phosphate. Several series of lcDNA samples over wide concentration ranges were prepared in this manner. All chemicals were the highest grade commercially available, and water was redistilled in glass.

Sample Preparation for Laser Diffraction and Light Microscopy. Samples used in laser diffraction experiments and visualized by polarized light microscopy were prepared on acid-cleaned microscope slides and coverslips. Routinely, a 10-μL lcDNA sample was placed between microscope coverslip and slide and sealed with a solubilized poly(methyl methacrylate) resin (Cornwell Corp., Stephens Scientific Division, Cytoseal 280). Samples prepared in this manner were stable for at least 7–10 days, and some displayed no signs of drying after several months. The mounting medium was allowed to set for 24 h prior to pitch measurements. This drying period also allowed the lcDNA sample to equilibrate prior to examination. In controlled drying experiments a small portion of the coverslip was left unsealed to allow slow evaporation of the lcDNA solutions. Sample thickness in these cases ranged from approximately 5 to 10 μm. To prepare thicker samples, a 100-μm-thick circular Nylon spacer (i.d. 15 mm) was placed on the microscope slide, and a 75-μL lcDNA sample was placed into the void volume under a coverslip.

Laser Diffraction. A 5-mW helium–neon (HeNe) laser (Uniphase) was mounted on an optical bench, and the polarized light was spatially filtered, and passed through a variable aperture and beam splitter, and then focused onto the sample for locally probing cholesteric pitch. The focused beam area was adjusted to a 10-μm diameter. For measurements of the average pitch the beam was defocused at the sample to a diameter greater than 3 mm. The sample (lcDNA on a microscope slide) was placed on a mechanical X-Y axis microscope slide translation stage and inserted into the light beam. Diffraction patterns were projected onto a 100 × 100 mm section of frosted glass and imaged with a Sanyo VDC-3900 color video camera focused through a 50-mm f3.5 Macro Minolta lens or photographed on Kodak Tmax 100 film (120 format) with a Mamiya RB 67 ProS medium format camera equipped with a 90-mm f3.7 lens and a 2× teleconverter. Video images were captured by using an Imaging Technologies Series 150 frame grabber driven by a Sun Microsystems Model 3/110 computer workstation, with software supplied by Hannaway and Associates. After each diffraction pattern was recorded, a swing-out lens (50×) was placed in the beam path between the focusing lens and the sample, and the reflected light that passed back through the beam splitter was photographed through a polarizer with an Olympus OM-2S 35-mm camera focused through a 4× Jena microscope projection lens. The swing-out lens could be moved back and forth in the beam path for optimum focus of the imaging camera. Images were recorded on Ektachrome 200 transparency film.

Polarized Light Microscopy. lcDNA samples were examined by polarized light microscopy utilizing a Nikon Optiphot-Pol microscope equipped with a UFX-II exposure monitor. Gross sample morphology was recorded at low magnification using the 4× and 10× objectives, but pitch measurements required higher magnification (40× objective). All images were recorded on Fijichrome 64 T, a tungsten color-balanced transparency film.

Magnetic Field Alignment. In the presence of a magnetic field the nematic director will tend to align relative to the field. The contribution of the field to the free energy of the nematic is

$$F_{mag} = {}^1/_2\chi_a(\mathbf{H}\cdot n)^2 \quad (1)$$

where **H** is the magnetic field and n is the symmetry axis for molecular orientation (i.e., the nematic director). Since DNA has a negative anisotropy in diamagnetic susceptibility, $\chi_a = \chi_\parallel - \chi_\perp$, the helices align perpendicular to an applied magnetic field,[6,20,21,31] and hence the *twist axis* of the cholesteric is parallel to the field. Alignment with the magnetic field is only at the expense of the preferred orientation on the bounding surfaces. For strongly anchored and viscous materials large magnetic aligning fields may be needed. Our samples aligned in 2–4 h in a 3.5-T NMR magnet, with the field parallel to the surface of the microscope slides. A 1.4-T field was found to be insufficient for alignment in 8–12 h.

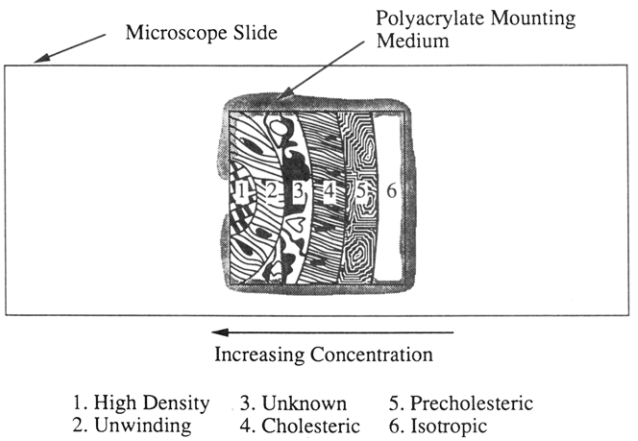

Figure 1. Diagrammatic representation of the sample in a *controlled drying* experiment. During the course of the experiment, a series of phases appear, which are represented as 1–6 in the figure. Phase 1, which is closest to the open section of coverslip, is the high-density phase illustrated in Figure 3i. Phase 2 is the unwinding cholesteric phase of high variable pitch (Figure 3f). Phase 3 is a region of complicated texture seen only in these controlled drying experiments, which were only performed in ammonium acetate buffer. Phase 4 is totally cholesteric and aligned well in a magnetic field (Figure 2i and 3c). Phase 5 is a biphasic region that is comprised of cholesteric and *precholesteric* regions (Figure 2f). Phase 6 is isotropic.

Results

Controlled Drying Experiments. Phase-transition zones were examined in detail by *controlled drying* experiments in which a 10-μL aliquot of concentrated DNA solution in the isotropic phase (100 mg/mL in 0.25 M ammonium acetate buffer, pH 6.5) was placed between a coverslip and microscope slide and partially sealed, leaving a 2–3-mm open section on one end. The direction of evaporation was thereby controlled, establishing an increasing concentration gradient of DNA (and salt) across the slide (Figure 1). (Note that the local C_D and C^+ are not well-defined in this case, but the phase sequence is representative of that for well-defined samples.)

A series of phases were observed, corresponding closely to those noted previously[18] (Figures 1–3). Samples were observed with and without alignment in a 3.5-T magnetic field. For the unaligned samples the phase progression with increasing concentration (as described in detail below) is isotropic → precholesteric → cholesteric → unwinding → multiple phases of higher density. Microscopic textures of samples not aligned in the magnetic field are illustrated in Figure 2. In aligned samples the same phase sequence was observed. The microscopic morphologies of the cholesteric and unwinding regions differed, however, because of field-induced changes in molecular orientations with respect to the viewer. These aligned samples are illustrated in Figure 3. Magnetic alignment had no discernable effect on the appearance of either the precholesteric or the high-density phases.

The morphologies of unaligned samples in controlled drying experiments are illustrated in Figure 2. Figure 2i shows the stable cholesteric phase. The bright bands are oily streaks, with the twist axis in the plane of the picture. The darker regions are cholesteric with planar alignment; the twist axis is mainly perpendicular to the picture. The black regions of Figure 2i exhibit no birefringence and are not liquid crystalline. Parts f and c of Figure 2 show cholesteric domains (Figure 2f) and spherulites in coexistence with the isotropic phase and the low-density anisotropic (*precholesteric*[18,19]) phase, which is not sufficiently birefringent to appear in the figures as reproduced here (but see below and Figure 5).

Magnetic alignment significantly altered the textures of the cholesteric and transition regions labeled in Figure 1 and thereby assisted in the location of phase boundaries and identification of phases. The morphologies of the aligned cholesteric phase are illustrated in parts c and f of Figure 3. Figure 3f is a high-magnification photomicrograph of the cholesteric phase illustrating the long pitch that occurs near the high-density transition. Quantitative measurements from photomicrographs and laser diffraction patterns indicate that the cholesteric pitch increases to approximately 8–10 μm in this region (see below). Immediately adjacent to the long-pitch region, in the direction of lesser DNA concentration, there occurred a region that appeared very disordered and remained unaligned in the magnetic field (labeled unknown in Figure 1). It is likely that in this region there is competition between the orienting effect of the glass surfaces and the magnetic field. There was no evidence of this region in the sealed samples, used for systematic pitch determination measurements (see below). It is possible that a combination of variation in supporting electrolyte concentration and DNA concentration results in a structure incompatible with an oriented phase. A fully cholesteric region occurred adjacent to the disordered region in the direction of lesser DNA concentration (Figure 3c). This region was well aligned in the magnetic field and displayed a pitch varying from 2.5 to 4 μm.

The various spatial measurements in these controlled drying experiments were obtained simultaneously by laser light diffraction and imaging. Figures 2 and 3 illustrate a sequence of photomicrographs of different regions in the drying slides, illustrating laser light diffraction patterns and laser light imaging of the same region, plus polarized microscope images from approximately the same regions. These data were extremely useful for interpreting the laser diffraction results. For example, in the high-density phase (Figure 3g–i), laser diffraction indicated a very long length scale of approximately 6 μm. Upon comparison with the simultaneous real image data, it was obvious that this long-length scale was associated with the striations seen in the high-density phases. We also determined that spherulites (Figure 2a–c), oily streaks (Figure 2g–i), and aligned cholesteric regions (Figure 3a–c) had the same ≈2-μm pitch by this simultaneous diffraction and imaging technique.

Experiments at Constant C_D and C^+. The observation of an apparently constant pitch of the cholesteric phase as the DNA concentration increased up to the transition region contrasted with previous studies of related systems. This suggested that a series of measurements at very well-defined DNA and supporting electrolyte concentrations was necessary.

Systematic measurements of the cholesteric helical pitch in lcDNA samples were made with 10-μL aliquots of lcDNA completely sealed between slide and coverclip. The lcDNA concentration utilized in these studies ranged from 150 to 400 mg/mL. The concentrations from 150 to 300 mg/mL fall approximately in the previously reported cholesteric lcDNA region determined for samples in 0.3 M NaCl and ammonium acetate.[18,19] Several supporting electrolyte concentrations and species were employed. With Na^+ as the counterion, samples with supporting electrolyte concentrations of 0.01, 0.1, and 1.0 M were prepared in 10-mg/mL C_D increments over the complete lcDNA concentration range. In experiments using NH_4^+ as the counterion, the supporting electrolyte concentration was

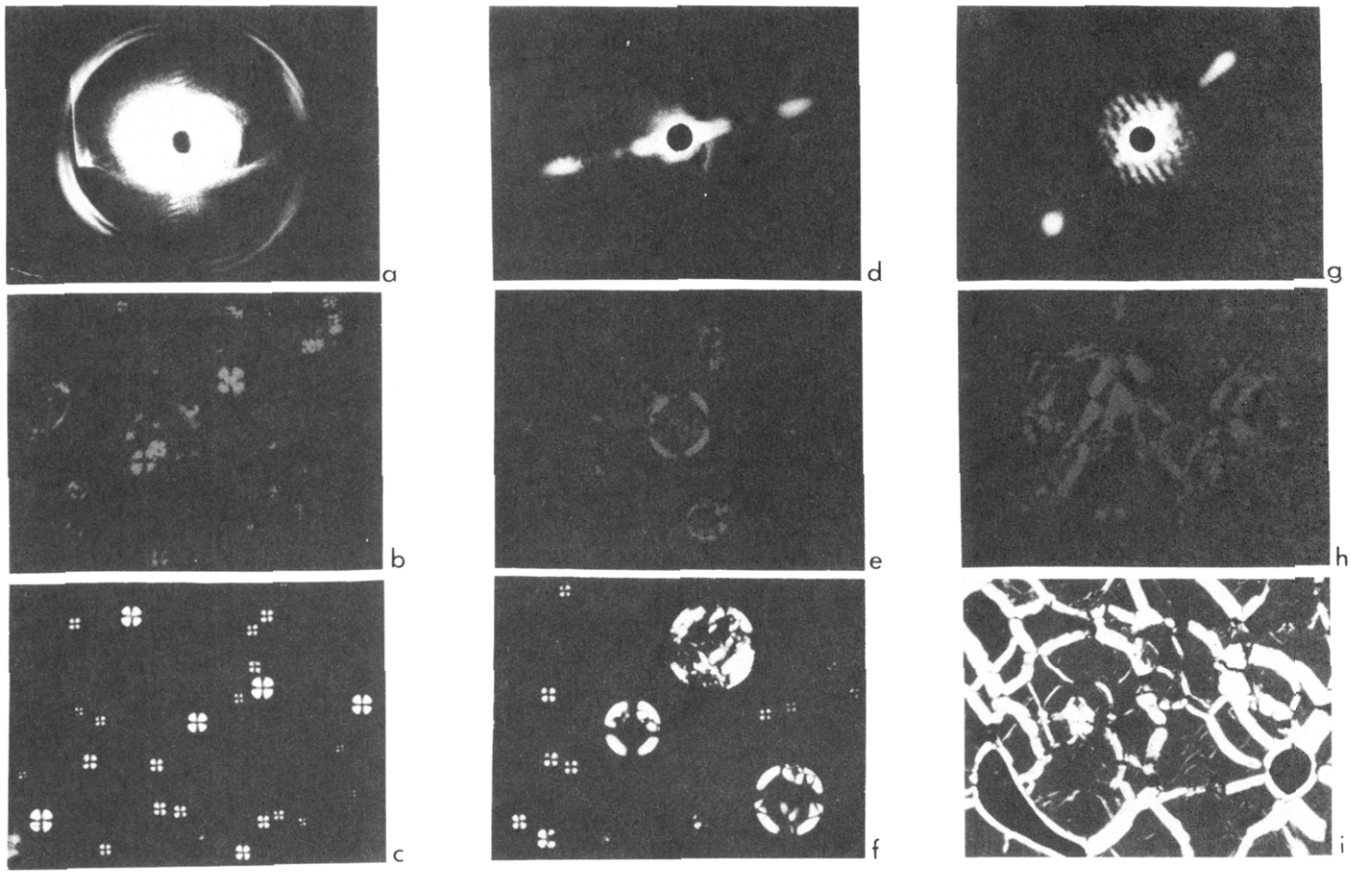

Figure 2. Laser light diffraction patterns, laser imaging patterns, and polarized light photomicrographs of various regions in *controlled drying* experiment. (a, d, and g) Laser diffraction patterns obtained from successive areas of the microscope slide in regions 4 and 5 of Figure 1. (b, e, and h) Laser imaging of the regions. (c, f, and i) Polarized light micrographs of areas near the regions where diffraction patterns were recorded.

0.25 M, and these samples were prepared in approximately 25-mg/mL C_D increments.

The measured pitch, P, of the cholesteric lcDNA phase up to the point of unwinding was essentially constant at a value of $P = P_c \equiv 2.2 \pm 0.2$ μm (Figure 4), regardless of the ionic species or concentration. A typical measurement was made by translating the sample in the focused laser beam until a distinct and oriented diffraction pattern was observed. The focus of the beam was adjusted to maximize the size of a coherence area in the diffraction pattern; thus, the source of diffraction was positioned at the minimum beam waist. The error bars in Figure 4 represent 1 standard deviation for each set of 25 measurements per point. Polarized light microscopic measurements (not illustrated) of the samples over the range in C_D of these data were consistent with the laser diffraction results. The microscopy studies revealed that cholesteric phase existed only in spherulites in the lowest C_D samples examined. At higher C_D, spherulites and isolated cholesteric regions coexisted, and at even higher C_D (≥220 mg/mL) the samples with $C^+ \geq 0.,1$ M were fully cholesteric. The measurements reported in Figure 4 therefore reflect the pitch in local regions of fully cholesteric domains.

For DNA concentrations between the onset of liquid-crystal formation (C_D = 130–160 mg/mL depending on C^+) and 100% cholesteric phase, there existed a weakly birefringent, but clearly liquid-crystalline, phase previously termed *precholesteric* in coexistence with isotropic and cholesteric liquid crystal. Strong nematic director fluctuations were observed in this region, consistent with a relatively low viscosity and orientational elasticity. In addition, there appeared to be a long and variable director rotation, as observed by depolarized light microscopy. This rotation is consistent with a cholesteric liquid-crystalline phase with long, variable pitch. The pitch of this rotation was observed, in thin samples, to be as high as 50 μm. Perhaps most significantly, in thicker (100 μm) samples of DNA at concentrations for which the precholesteric and cholesteric phases coexisted, the pitch was observed to decrease continuously to the stable ≈2-μm pitch at precholesteric/cholesteric boundaries (Figure 5). The precholesteric phase was so weakly birefrigent that, even in broad-beam diffraction experiments, no other quantitative measurements of pitch could be obtained.

For cholesteric samples near the transition to the high-density phase, alignment produced regions of varying pitch. Consistent measurements were more difficult to obtain than was P_c for the stable cholesteric phase. Measurements of P obtained both by laser light diffraction and by polarized light microscopy are illustrated in Figure 6. As C_D is increased above 300 mg/mL, the pitch dramatically increased regardless of the counterion species (Na^+ or NH_4^+), though the critical C_D for initiation of the divergence was less when NH_4^+ was the counterion species. All Na^+ samples exhibited a pitch of about 2.1 μm at C_D = 270 mg/mL, indicating that the unwinding of the cholesteric phase had not begun, whereas for 0.25 M NH_4^+ at 280 mg/mL, the pitch had increased to 3.6 μm. Since each point plotted represents an average of approximately 25 single measurements for each sample, the difference in onset is significant.

Discussion

Polyelectrolyte Character of DNA. Attempts at understanding the fundamental physics of rodlike DNA

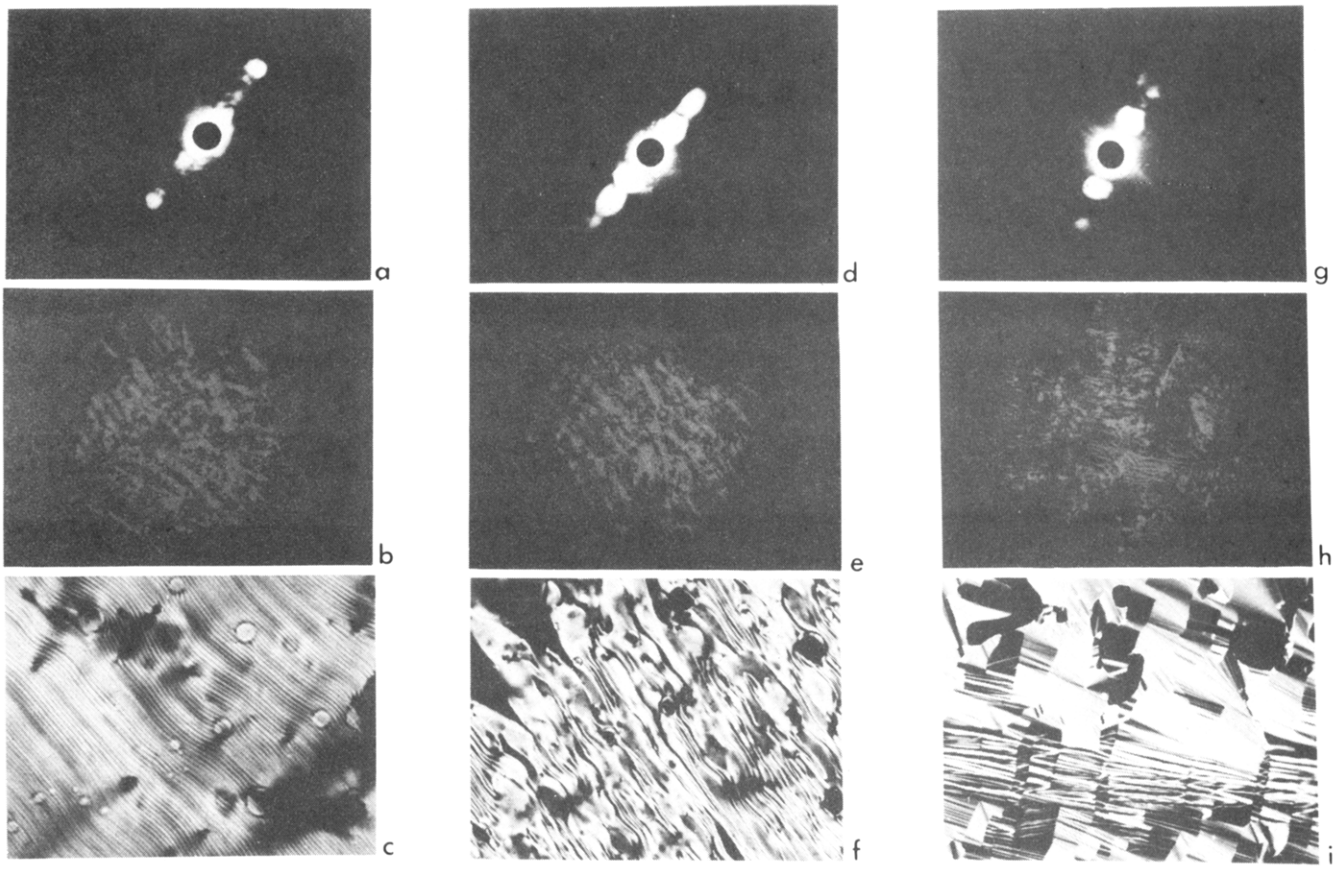

Figure 3. Diffraction and imaging of patterns similar to Figure 2. (a, d, and g) Laser diffraction patterns obtained after magnetic field alignment from areas 4, 2, and 1, respectively, in Figure 1. (b, e, and h) Laser imaging after magnetic field alignment of the areas that gave rise to the diffraction patterns in a, d, and g. (c, f, and i) Polarized light micrographs of the same areas.

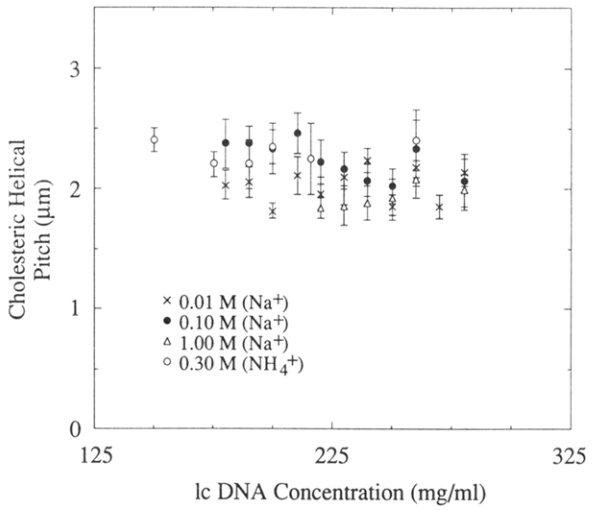

Figure 4. Change in the cholesteric lcDNA helical pitch as a function of lcDNA concentration and counterion concentration and species.

molecules in aqueous solutions of 1:1 electrolytes are aided by a description of the DNA and its counterion atmosphere suggested by Schellman and Stitger.[34,35] The DNA ionic double layer is described as consisting of three regions. At large distances from the helix axis (>2.0–2.5 nm), the electrostatic potential can be approximated (at moderate to high C^+) by treating the DNA as a rigid, uniformly charged rod. The electrostatic potential surrounding the rod is assumed to be cylindrically symmetric, and the interaction potential is described adequately by the Debye–Hückel approximation in the content of the counterion condensation theory for strong polyelectrolytes.[38,39] The anisotropy along the axis of the rods associated with the twisted double helix should not have a significant influence on the self-assembly of ordered phases in this limit of relatively low C_D. At closer distances to the helix axis, when the interaction potential between charges becomes greater than k_BT (the Boltzmann constant times temperature), the full nonlinear Poisson–Boltzmann relation is required to describe the electrostatic potential. In this intermediate or Gouy–Chapman region (approximately 1.3 nm $< r <$ 2.0 nm) cylindrical symmetry has been widely adopted as an approximation,[34–36,38,39] but recent Monte Carlo calculations incorporating the explicit DNA charge distribution have shown that the electrostatic potential reflects the double-helical geometry at these distances, despite charge shielding by counterions.[40–43] The innermost region of the double layer has been termed the Stern layer, and in this layer the interaction potential is determined by all of the intrinsic molecular structure. This complicated set of interaction regimes may be related, in part, to the rather complex DNA phase behavior observed. At high enough C_D neighboring DNA molecules will be sufficiently close that the structural anisotropy of the major and minor grooves and the distribution of counterions bound to the rods will profoundly affect intermolecular interactions and therefore the structures of ordered phases.

Contributions to Nematic Twist. The contributions to twist in chiral lyotropic polymer liquid crystals are still incompletely understood, particularly for polyelectrolytes. When intermolecular separations are small or the molecules are long, van der Waals forces are expected to contribute. At least two groups[44,45] have described how a van der Waals rod–rod interaction could give rise to a twist if the rods have helical anisotropy. As discussed by Maret and co-workers,[20,21] the van der Waals binding

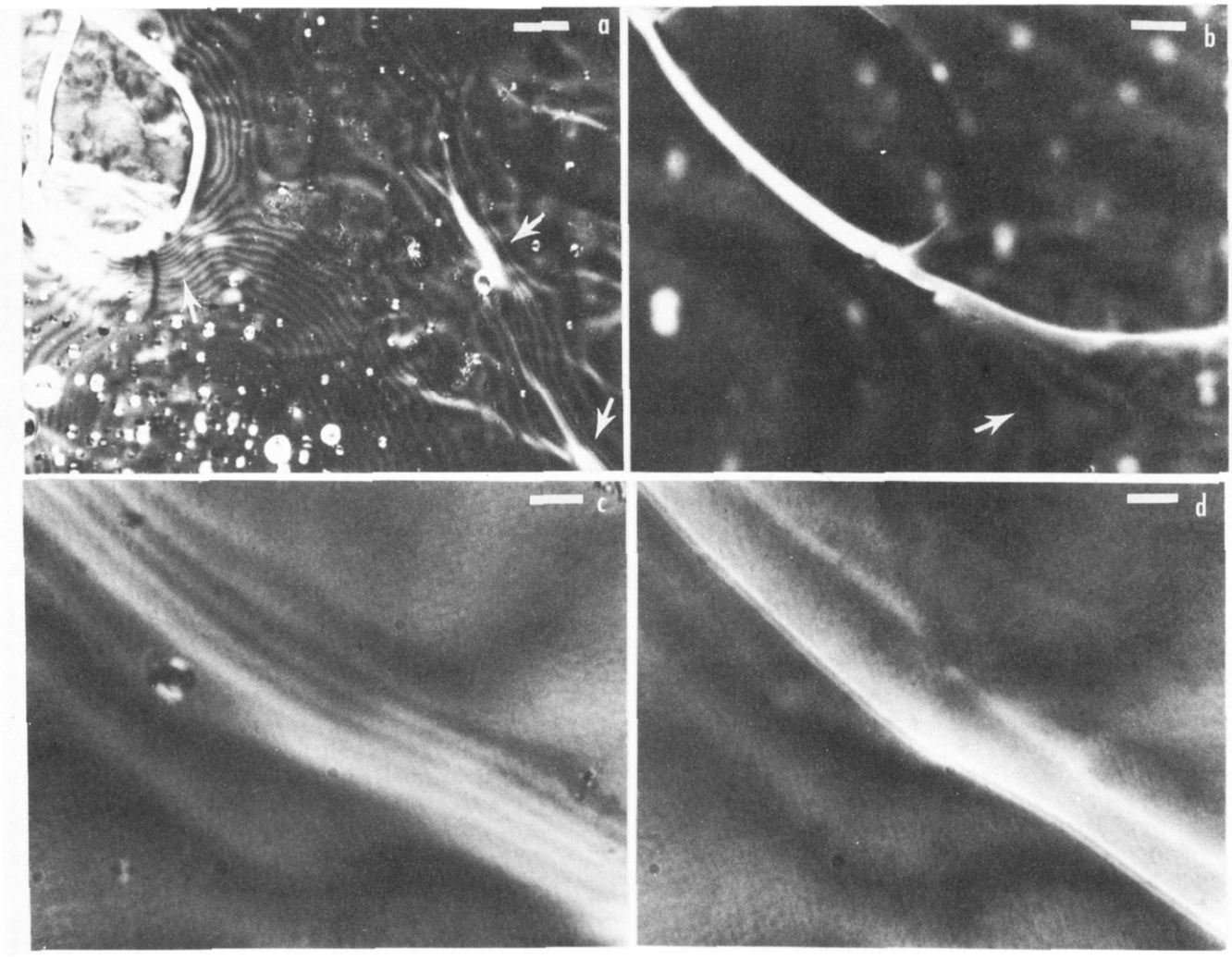

Figure 5. Photomicrographs illustrating the helical pitch changes at cholesteric/precholesteric liquid-crystalline phase boundaries in 100-μm-thick samples. (a) Low-magnification micrograph showing the pitch change at the cholesteric/precholesteric boundary (white arrows). Present in the sample are numerous spherulites and cholesteric "oily streaks". Bar represents 200 μm. (b) Medium-magnification micrograph showing the collapse of the precholesteric pitch onto a cholesteric oily streak (white arrow). Bar represents 100 μm. (c and d) High-magnification views of the same viewfield at different focal planes. The precholesteric phase in (c) has a pitch of 10–30 μm, which decreases to a constant 2–3 μm at a lower focal plane in (d). Bar represents 25 μm.

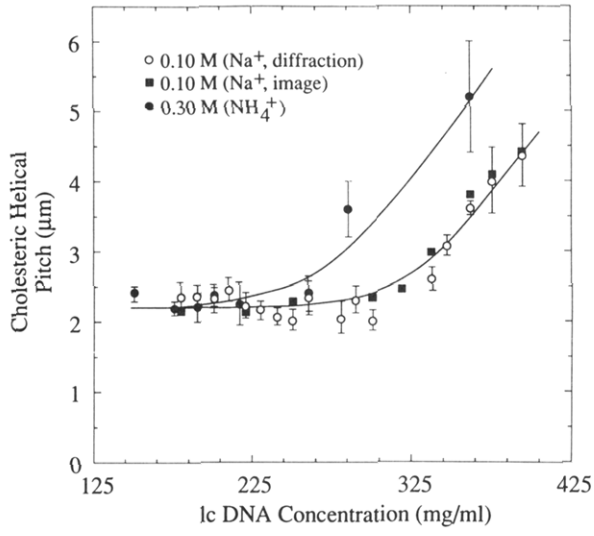

Figure 6. Change in the cholesteric lcDNA helical pitch as the concentrations are greatly increased over those shown in Figure 4.

energy increases with rod length. For the intermolecular separations and fragments as short as those studied here, the van der Waals contribution is expected to be much less than k_BT.[20,39]

The theory of Odijk[46] explicitly predicts the pitch of a *nonelectrolyte* polymer cholesteric using virial theory in which the chiral interactions are treated as a perturbation on the excluded-volume effect. The pitch is determined by balancing the chiral forces inducing twist against elastic forces favoring the untwisted (nematic) state. The predicted pitch for long, rigid chiral rods is

$$P \simeq (\Delta D \rho_L)^{-1} \tag{2}$$

where Δ is the thickness of a thin helical thread around the rod of thickness D and ρ_L is the number density of rods.

Electrostatic repulsions are expected both to provide a major contribution to the twist and to resist anisotropic phase formation of a polyelectrolyte. The lowest free energy configuration for two charged rods is perpendicular. This is seen by explicitly expressing the dependence of the Debye–Hückel electrostatic pair interaction potential, ω, on ϕ, the relative orientation of two rods measured perpendicular to the line connecting rod centers

$$\omega \propto e^{-\kappa x}/\sin \phi \tag{3}$$

where κ is the Debye screening length proportional to (ionic strength)$^{1/2}$ and x is the closest distance between rods.[47] Using this, Stroobants et al.[47] calculated the effects

of twist on phase boundaries, concluding that twist increases the critical concentration for anisotropic phase formation.

To our knowledge, the contributions of electrostatic interactions to the magnitude of the cholesteric pitch of a rodlike strong polyelectrolyte have not been described quantitatively. Two predictions appear to follow qualitatively from eq 3. Increasing the supporting electrolyte concentration *at constant DNA concentration* should *increase* the pitch because of greater charge screening. On the other hand, since the electrostatic potential increases with decreasing rod spacing, the pitch should decrease if the polyelectrolyte concentration is increased *at constant ionic strength*. (It should be noted that the latter condition cannot be easily met for concentrated solutions of a strong polyelectrolyte, since the macroion typically contributes significantly to the ionic strength at the concentrations required for phase formation.) Further, for a strong polyelectrolyte the electrostatic potential rises abruptly in the Guoy–Chapman region, more abruptly than the Debye–Hückel potential; hence, the decrease in pitch is expected also to be abrupt as the average intermolecular separation becomes small. The tendency toward a decrease in pitch will be augmented by the excluded-volume effect described by Odijk and additional electrostatic effects if the polyelectrolyte is chiral.

Precholesteric Phase and Precholesteric to Cholesteric Transition. Our observations of liquid-crystalline DNA phases appear qualitatively consistent with the above hypotheses of polyelectrolyte behavior. We have confirmed previous observations that the lowest density anisotropic DNA phase is very weakly birefrigent, exhibiting irregular periodicities on 10–50-μm length scales. Slight twist is expected to arise from the long-range electrostatic interaction described by a Debye–Hückel potential, as noted by Stroobants et al.[47] Systematic measurements of the pitch were not possible, but variations in the local C_D and C^+ appeared to significantly alter the periodicity. As C_D was increased, the $\approx$2-μm-pitch cholesteric phase first appeared as small spherulites and then expanded to globules or "islands" in the precholesteric phase. Particularly intriguing were the observations, in thick samples, of cholesteric oily streaks of pitch $\approx P_c$ apparently opening into optically birefrigent bands of spacing as high as 50 μm (Figure 5). This behavior is consistent with the conclusion that the precholesteric phase is a twisted nematic of very long pitch. In addition, the DNA concentration corresponding to onset of the cholesteric phase in 0.01 and 0.1 M supporting electrolyte was $\approx$200 mg/mL, corresponding to an average interhelical center-to-center spacing $\approx$ 50 Å. At this separation the DNA rods, as effective particles, begin to (hypothetically) overlap; i.e., the electrostatic potential between rods is expected to rise steeply and may drive an abrupt increase in twist angle between helices (decrease in pitch).

Cholesteric Phase. By contrast with the low-density "precholesteric" phase, the pitch of the obviously cholesteric phase observed with these modest length DNA fragments was remarkably independent of both DNA and supporting electrolyte concentration. At concentrations below about 220 mg of DNA/mL the solutions were biphasic. Further, Strzelecka and Rill showed that the phase behavior of DNA solutions in a 0.01 M supporting 1:1 electrolyte is more complex than that observed at higher supporting electrolyte concentrations, and a small amount of isotropic phase persists up to the cholesteric/high-density phase boundary.[37] Under these conditions the concentration of the cholesteric phase is expected to remain constant although the proportions of the phases vary. Accordingly, there is no driving force for a pitch change with increasing C_D.

Solutions with $C^+ \geq 0.1$ M appeared completely cholesteric over the C_D range of about 220 to 300–330 mg/mL. Furthermore, no systematic change in pitch was noted on increasing the supporting electrolyte concentration from 0.01 to 1.0 M over this concentration range. The constancy of the measured value of $P = P_c \equiv 2.2 \pm 0.1$ μm is surprising since the center-to-center distance between helices is approximately 50 Å at a concentration of 220 mg/mL and 41 Å at a concentration of 330 mg/mL (calculated assuming hexagonal packing of hard spherocylinders, 500 Å long with a radius of 12.5 Å). In the simplest case that the angle of rotation, ϕ, between adjacent molecules along the twist axis was determined solely by a steric interaction related to the threaded shape of the rod, then ϕ would be independent of C_D and the macroscopic cholesteric pitch P would decrease in proportion to the decrease in inter-rod distance or from 2.2 μm at C_D = 220 mg/mL to $\approx$1.8 μm at C_D = 330 mg/mL. Assuming a simple inverse relationship between C_D and the pitch according to the Odijk formalism for nonelectrolyte rods, an increase in DNA concentration from 220 to 330 mg/mL should be accompanied by an $\approx$30% decrease in pitch from 2.2 to 1.5 μm. Electrostatic interactions should further decrease the pitch.

The constancy of the pitch in this DNA concentration range may be attributed in part to the contribution of some fraction of the DNA counterions to the effective ionic strength. There is no precise means to estimate this fraction for such concentrated DNA solutions, but it is unlikely to be less than the 24% predicted by Manning's theory for dilute solutions.[38,39] An increase in effective ionic strength necessarily accompanied an increase in C_D and may have moderated the expected decrease in pitch due to electrostatic interactions. The tendency of the pitch to unwind prior to high-density phase formation may also partly compensate electrostatic contributions to twist over this narrow DNA concentration range (see below). These effects do not explain, however, the identical pitches observed at the same overall DNA concentrations in 0.01, 0.1, and 1.0 M NaCl.

Helical pitch measurements were previously reported for cholesteric liquid-crystalline solutions of polydisperse, double-helical polyribonucleotide mixtures in two independent investigations.[20-26] These reports differ from ours in that significant decreases in cholesteric pitch with increasing polyribonucleotide concentration were measured. Iizuka examined mixtures of poly(A)·poly(U) and poly(A)·2poly(U), rodlike polyribonucleotide complexes, which were found to form cholesteric phases with a pitch decreasing from 5 to 1 μm for A·U and from 10 to 2 μm for A·2U, over a concentration range of 60–200 mg/mL. They measured the pitch dependence on concentration and calculated a decrease as $P \propto C_D^{-1}$. Maret and coworkers[20,21] studied concentration effects on the cholesteric helical pitch in solutions of ribonucleic acid molecules, primarily poly(A)·poly(U), with a mean length of 1700 Å. They found the onset of the liquid-crystalline phase at about C_D = 70 mg/mL and measured a decrease in pitch from 3.2 to 2.0 μm over the concentration range 70–200 mg/mL. Fitting these data to a power law, they found $P \propto C_D^{-1/2}$.

The lower concentration for onset of cholesteric phase formation observed by Iizuka and Maret et al. compared to that reported here for $\approx$500-Å DNA fragments is

consistent with the greater length of the ribonucleic acid duplexes examined. The origins of the inconsistencies between the concentration dependence of the cholesteric pitch reported here and the results discussed above are uncertain but may be due to differences in the degree of length dispersity between the samples examined by the three groups. van der Waals and electrostatic contributions to twist are length dependent. Stroobants et al.[47] showed that long rods are always more ordered in a nematic phase than shorter rods, and Lekkerkerker et al.[48] showed that a solution of rodlike particles of two lengths would phase separate, with a higher mole fraction of long rods in the anisotropic phase. The extension of Flory's lattice statistics approach to the I–A transition in solutions of rods with more than one length also shows that higher axial ratio rods will preferentially partition into the anisotropic phase.[49] A dependence of the cholesteric pitch on DNA concentration for polydisperse samples would, therefore, not be surprising.

Unwinding of the Cholesteric and Formation of High-Density Phases. There is an interaction that tends to untwist a cholesteric. As the concentration increases, the local packing density increases. At a particular concentration the effective volume excluded by the rods is reduced by increasing the pitch. The system free volume, hence the entropy, increases by allowing one rod to occupy the depression between two other rods. The observation of constant pitch as C_D increases can be rationalized as a balancing of the competition between the steric and electrostatic interactions tending to increase twist and the system entropy enhancement tending to reduce twist. High-density DNA phases were previously reported by Strzelecka et al.[19] and Livolant.[28] Recent optical birefringence measurements made by Livolant and co-workers[33] showed that DNA solutions eventually form a high-density columnar phase. The existence of other high-density phases, indicated in the present studies by changes in the morphology observed by polarized light microscopy with increases in DNA concentration above that required for first observation of the high-density phase, coupled with the recent observation of a hard-rod smectic phase in Tobacco Mosaic Virus,[50] suggests a complete understanding of the high-density region of the DNA phase diagram is lacking.

Changes in the sample morphology consistent with untwisting of the cholesteric were observed as C_D was increased and approached the concentration for high-density phase formation. Magnetically aligned samples subjected to controlled drying were used to obtain initial measurements of the cholesteric pitch change with concentration. In the transition region these samples exhibited a continuous increase in pitch from about 2.5 to 4 μm. With further increase in C_D, the morphology became disordered and difficult to interpret. At still higher C_D, the morphology once again appeared cholesteric, with the twist axis again parallel to the direction of applied magnetic field and varying from 8 to 10 μm. These microscopic observations provided additional motivation for systematic pitch measurements on static samples. Measurements in sealed cells, made by both diffraction and image analysis, showed that the pitch increased continuously with increasing DNA concentration above 300 mg/mL; a disordered region was not observed.

Creation of a higher density liquid-crystal phase from a cholesteric phase requires unwinding of the twist axis. If there were no unwinding, columnar or smectic ordering would be accompanied by extensive formation of defects with a high cost in distortion free energy. For lyotropic liquid crystals the concentration of rods, C_D, is the appropriate thermodynamic variable to describe the critical properties of the transition. The analogy between C_D, the critical parameter for lyotropics, and T, the critical parameter for thermotropic phase transitions, can be made quantitative.

In general the twist free energy of a cholesteric is[51]

$$F_T = {}^1/_2 K_{22}(\mathbf{n}\cdot\nabla \times \mathbf{n} + q_o)^2 \quad (4)$$

where K_{22} is the Frank orientational elastic constant for twist and q_o is the wavevector for the preferred cholesteric pitch $P_o(C_D) = 2\pi/q_o$. Since $q_o = K_2/K_{22}$, where K_2 is the elastic modulus associated with a twist contribution to the free energy linear in gradients of $\mathbf{n}$, the critical behavior of P_o will be the same as the critical behavior of K_{22}. Near the transition, the effective twist elastic constant $K_{22}(Y) = K_{22} + \delta K(Y)$, where Y represents either T or C_D. The change δK can be written as $\delta K \sim k_B T\xi/a^2$, where ξ is the correlation length for pretransitional ordering of the high-density phase in the cholesteric phase and a is a molecular length. For the thermotropic phase transition, $Y = T$ and the correlation length diverges as $\xi = \xi_o(T/T_c - 1)^{-\nu}$, where T_c is the extrapolated second-order transition temperature and ν is the critical exponent estimated to be 0.67.[52] Measurements of the intrinsic twist viscosity,[53] the pitch,[54] and elastic constant measurements[55] verify this exponent. For the lyotropic transition, $Y = C_D$ and the correlation length diverges as $\xi = \xi_o(C_D/C_D^* - 1)^{-\nu}$, where C_D^* is the extrapolated critical concentration for the transition. We do not attempt to fit our data with this form, since the change in reduced concentration ($C_D/C_D^* - 1$), over which we measure the divergence, is less than a single decade. It may not be possible to improve on this range, if C_D^* is significantly greater than the concentration for first formation of the high-density phase.

In summary, the lowest density anisotropic phase, termed precholesteric, appears to be a twisted nematic phase with large pitch dependent on the local density of DNA. In the vicinity of coexisting higher density cholesteric phase the pitch of the precholesteric phase apparently continuously decreases to the value of 2.2 μm observed for the cholesteric phase. This abrupt pitch change may be related to the sharp increase in electrostatic potential and introduction of chirality into the electrostatic potential expected when the average center-to-center helical rod separation approaches the effective DNA diameter. The pitch of the fully cholesteric phase was independent of both average DNA concentration from approximately 220 to 330 mg/mL and supporting electrolyte concentration, C^+, from 0.1 to 1.0 M. The failure of the pitch to decrease with increasing C_D may relate, in part, to the increased charge screening accompanying the increase in the effective ionic strength, but the constancy of pitch with increasing C^+ at constant C_D remains unexplained. At higher concentrations of DNA, divergence of the twist was observed as the cholesteric → high-density phase transition was approached. The onset C_D of this divergence depends on the added ionic species but apparently not strongly on the supporting electrolyte concentration. Untwisting is an expected precursor for the formation of more ordered higher density phases to minimize defect formation (maximize the free volume) and may compete with the electrostatic twisting effect, thereby maintaining the cholesteric pitch constant over a relatively narrow concentration range.

Acknowledgment. We thank Maxwell Godfrey for assistance in programming and operating the image

processor. This research was supported in part by the MARTECH program, funded by the State of Florida, and by NIH Grant GM 37098.

References and Notes

(1) Mazur, G. D.; Regier, J. C.; Kafatos, F. C. In *Insect Ultrastructure*; King, R. C., Adair, H., Eds., Plenum: New York, 1982; Vol. 1, p 150.
(2) White, J. L. *J. Appl. Polym. Sci., Appl. Polym. Symp.* **1985**, *41*, 3.
(3) Vian, B. In *Cellulose and Other Natural Polymer Systems. Biogenesis, Structure, and Degradation*; Brown, R. M., Jr., Ed.; Plenum: New York, 1982; p 23.
(4) Rill, R. L. In *Supramolecular Structure and Function*; Pifat-Mrzljak, G., Ed.; Plenum: New York, 1988; p 166.
(5) Baer, E.; Hiltner, A.; Keith, H. D. *Science* **1987**, *235*, 1015.
(6) Rill, R. L.; Livolant, F.; Aldrich, H. C.; Davidson, M. W. *Chromosoma*, in press.
(7) Earnshaw, W. C.; Casjens, S. R. *Cell* **1980**, *21*, 319.
(8) Onsager, L. *Ann. N.Y. Acad. Sci.* **1949**, *51*, 627.
(9) Flory, P. J. *Proc. R. Soc. London, A* **1956**, *234*, 60.
(10) Flory, P. J. *Proc. R. Soc. London, A* **1956**, *234*, 73.
(11) Lasher, G. *J. Chem. Phys.* **1970**, *53*, 4141.
(12) Alben, R. *Mol. Cryst. Liq. Cryst.* **1971**, *13*, 193.
(13) Odijk, Th. *Macromolecules* **1986**, *19*, 2313.
(14) Robinson, C. *Tetrahedron* **1961**, *13*, 219.
(15) Mishra, R. K. *Mol. Cryst. Liq. Cryst.* **1975**, *29*, 201.
(16) Hilliard, P. R., Jr.; Smith, R. M.; Rill, R. L. *J. Biol. Chem.* **1986**, *261*, 5992.
(17) Rill, R. L. *Proc. Natl. Acad. Sci. U.S.A.* **1986**, *83*, 342.
(18) Strzelecka, T. E.; Rill, R. L. *J. Am. Chem. Soc.* **1987**, *109*, 4513.
(19) Strzelecka, T. E.; Davidson, M. W.; Rill, R. L. *Nature* **1988**, *331*, 457.
(20) Senechal, E.; Maret, G.; Dransfeld, K. *Int. J. Biol. Macromol.* **1980**, *2*, 256.
(21) Maret, G.; Dransfeld, K. In *Topics in Applied Physics*; Herlach, F., Ed.; Springer: New York, 1985; p 143.
(22) Iizuka, E. *Polym. J.* **1977**, *9*, 173.
(23) Iizuka, E.; Kondo, Y. *Mol. Cryst. Liq. Cryst.* **1979**, *51*, 285.
(24) Iizuka, E. *Polym. J.* **1978**, *10*, 237.
(25) Iizuka, E. *Polym. J.* **1978**, *10*, 293.
(26) Iizuka, E. *J. Appl. Polym. Sci., Appl. Polym. Symp.* **1985**, *41*, 131.
(27) Livolant, F. *Eur. J. Cell Biol.* **1984**, *33*, 300.
(28) Livolant, F.; Bouligand, Y. *J. Phys. (Paris)* **1986**, *47*, 1813.
(29) Livolant, F. *J. Phys. (Paris)* **1986**, *47*, 1605.
(30) Livolant, F. *J. Phys. (Paris)* **1987**, *48*, 1051.
(31) Brandes, R.; Kearns, D. R. *Biochemistry* **1986**, *25*, 5890.
(32) Brian, A. A.; Frisch, H. L.; Lerman, L. S. *Biopolymers* **1981**, *20*, 1305.
(33) Livolant, F.; Levelut, A. M.; Doucet, J.; Benoit, J. P. *Nature* **1989**, *339*, 724.
(34) Schellman, J. A.; Stitger, D. *Biopolymers* **1977**, *16*, 1415.
(35) Stitger, D. *Biopolymers* **1977**, *16*, 1435.
(36) Le Bret, M.; Zimm, B. H. *Biopolymers* **1984**, *23*, 271.
(37) Strzelecka, T.; Rill, R. L. *Biopolymers*, in press.
(38) Manning, G. S. *Q. Rev. Biophys.* **1978**, *11*, 179.
(39) Manning, G. S. *Acc. Chem. Res.* **1979**, *12*, 443.
(40) Clementi, E.; Corongiu, G. *Biopolymers* **1982**, *21*, 763.
(41) Pack, G. R.; Wong, L.; Prasad, C. V. *Nucleic Acids Res.* **1986**, *14*, 1479.
(42) Troll, M.; Zimm, B. H. *Biopolymers* **1988**, *27*, 1711.
(43) Jayaram, B.; Sharp, K. A.; Honing, B. *Biopolymers*, in press.
(44) Goosens, W. J. A. *Mol. Cryst. Liq. Cryst.* **1971**, *12*, 237.
(45) Samulski, T. V.; Samulski, E. T. *J. Chem. Phys.* **1977**, *67*, 824.
(46) Odijk, T. *J. Phys. Chem.* **1977**, *91*, 6060.
(47) Stroobants, A.; Lekkerkerker, H. N. W.; Odijk, Th. *Macromolecules* **1986**, *19*, 2232.
(48) Lekkerkerker, H. N. W.; Coulon, Ph.; Van der Haegen, R.; Deblieck R. *J. Chem. Phys.* **1984**, *80*, 3427.
(49) Flory, P. J.; Abe, A. *Macromolecules* **1978**, *11*, 1119. Abe, A.; Flory, J. *Ibid.* **1978**, *11*, 1122; Flory, P. J.; Frost, R. S. *Ibid.* **1978**, *11*, 1126. Frost, R. S.; Flory, P. J. *Ibid.* **1978**, *11*, 1134.
(50) Wen, X.; Meyer, R. B.; Casper, D. L. D. *Phys. Rev. Lett.* **1989**, *63*, 2760.
(51) We follow the discussion in: Chandrasekhar, S. *Liquid Crystals*; Cambridge University Press: New York, 1977; p 311.
(52) de Gennes, P.-G. *Solid State Commun.* **1972**, *10*, 753; *Mol. Cryst. Liq. Cryst.* **1973**, *21*, 39.
(53) Huang, C. C.; Pindak, R. S.; Flanders, P. J.; Ho, J. T. *Phys. Rev. Lett.* **1974**, *33*, 400.
(54) Pindak, R. S.; Huang, C. C.; Ho, J. T. *Solid State Commun.* **1974**, *14*, 821.
(55) Cheung, L.; Meyer, R. B.; Gruler, H. *Phys. Rev. Lett.* **1973**, *31*, 349.